Blue Laser Conduction Welding of Dissimilar Cu and Al Sheets

This work demonstrates that blue laser has great potential for joining 0.6 mm Cu and 0.6 mm Al sheets for new energy applications

BY Z. TANG, H. YANG, L. WAN, P. REN, X. ZHANG, Y. WU, H. WANG, AND H. WANG

Abstract

Joining Cu-Al with 0.6 mm is important for the high-power density battery in the new energy field. Low laser absorptivity is a challenge in Cu-Al welding with conventional infrared laser at around 1000 nm wavelength, where keyhole welding is necessary. It is difficult to control welding qualities in keyhole welding due to the intense flow and violently changing absorption rate. At 450 nm wavelength, Cu and Al have high laser absorptivity which has the potential to implement stable conduction welding. Therefore, this work adopted a blue laser welding system, and for the first time, realized the conduction welding of 0.6 mm Cu and 0.6 mm Al sheets. The welding process, surface appearance, mechanical properties, and electrical properties were investigated. The results showed that high-power (1950 W) could effectively realize stable Cu-Al conduction welding without spatters, and the welding speed could reach 40 mm/s. Compared with an infrared laser, the blue laser could weld Cu-Al using the form of Cu on top and Al on bottom, which was beneficial for a wide process window and stable welding process. A larger bead width and more consistent intermetallic compound thickness resulting from the blue laser were conducive to performance improvement. In addition, the relationship between welding parameters, molten pool characteristics, and process qualities was built. It provided a possibility to control the welding quality under the influence of strong heat accumulation and high thermal conductivity. This work demonstrated that blue laser has great potential in joining Cu-Al for new energy applications.

Keywords

- Laser Welding
- Blue Laser
- Battery Tab
- Molten Pool
- Electrical Property

Introduction

Cu and Al are important metal materials in industry because of their high thermal and electrical conductivity (Ref. 1). Laser welding, joining the materials, has obvious significance in industrial production because of high stability, processing efficiency, electrical property, and mechanical property (Refs. 2, 3). However, due to the high reflectivity, single-sided laser beam welds between thin (< 1.0 mm) sheets of Al and Cu in a lap joint configuration, namely laser welding Cu-Al, is a big challenge (Ref. 4). When applying the conventional infrared laser, the laser absorptivity for Cu is low to about 3%, and that for Al is about 5% (Refs. 5, 6). It hinders the development of many key industries, especially the new energy field where there are massive Cu and Al applications in lithium battery tabs, busbars, etc.

Some researchers have tried to join Cu-Al with an infrared laser. Hollatz et al. (Ref. 7) and Jarwitz et al. (Ref. 8) applied the continuous infrared laser with spatial beam oscillation to welding Cu-Al relying on keyhole welding. They found that when the aluminum was on the top and copper was on the bottom, there were many pores with larger sizes; instead, though the pores were smaller, the process window was very narrow. Dimatteo et al. (Ref. 9) also realized the welding of Cu and Al sheets by continuous infrared laser welding with circular laser beam oscillation. Except for the continuous infrared laser, Ascari et al. (Ref. 10) used the short pulse infrared laser welding to join Cu-Al and could make them in a low fusion state. Lerra et al. (Ref. 22) further optimized the process parameters of the short pulse infrared laser welding, and it could reach a rela-
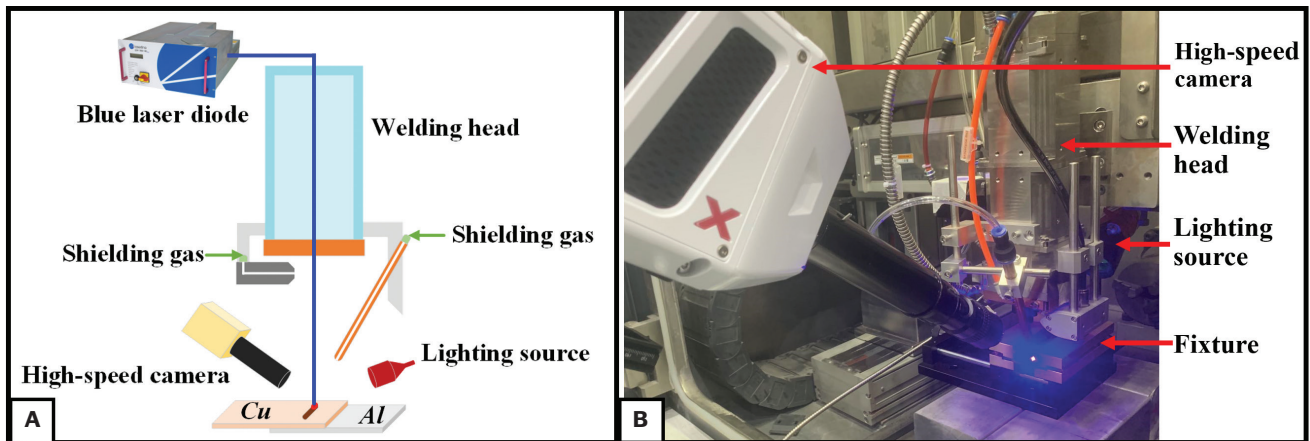
Fig. 1 — A — Experimental schematic diagram; B — photo of the 2000 W blue laser welding system.

Table 1 — Chemical Composition of Commercially Pure Cu (T1)

Chemical Element	Cu	P	Fe	Ni	Pb	Sn	S	Zn
Mass Fraction (wt-%)	≥ 99.50	≤ 0.001	≤ 0.005	≤ 0.002	≤ 0.003	≤ 0.002	≤ 0.005	≤ 0.005

tively larger depth. Currently, the main problem of infrared laser welding Cu-Al is that to avoid the low laser absorptivity, the keyhole welding mode is necessary which can improve the laser absorptivity through multiple reflections. However, the keyhole welding increases the instability of the welding process. Meanwhile, the Al on top and Cu on bottom is also a way to increase the laser absorptivity. However, it leads to a narrow process window because of the balance of mechanical and electrical properties. Therefore, it is a challenge to achieve high stability and reliability in welding dissimilar Cu and Al sheets.

The blue laser diode with a wavelength of 450 nm was developed in 1994 (Refs. 11, 12), which has a much higher absorptivity than the conventional infrared laser for processing high-reflectivity metal materials, such as Cu and Al (Refs. 13, 14). For Cu, the laser absorptivity can reach about 65%; for Al, the absorptivity can also achieve nearly 15% (Refs. 5, 6). Therefore, the blue laser is a very important and promising energy source in welding. Sadeghian et al. (Ref. 15) applied a 1500 W blue laser to join the 0.3 mm thick Ni-coated Cu and 0.6 mm thick Ni-coated mild steel sheets and achieved a well mechanical property after process parameter optimization. Yuan et al. (Ref. 16) compared the welding effect of blue laser welding and circular infrared laser oscillation welding when welding 1 mm 7075-T6 aluminum alloy and 3 mm carbon fiber reinforced polyetheretherketone. The result showed that the weld bead resulting from the blue laser had fewer defects and better mechanical properties. Tang et al. (Ref. 17) applied the blue laser to weld the electrical steels and analyzed the molten pool characteristics. They found the large spot, flat top, and

blue laser had the advantages of the self-stabilizing ability on welding laminated sheets. For welding Cu-Al, Britten et al. (Ref. 18) preliminarily applied a 1500 W blue laser diode of Laserline GmbH for welding Cu-Al sheets. The result showed the possibility of the blue laser in welding Cu-Al. At present, the blue laser has shown its advantage in welding for the new energy field. However, there is still a lack of systematic research on Cu-Al welding with blue laser for analyzing the welding process and characterizing the properties. It is not clear how the blue laser influences the welding of dissimilar Cu and Al sheets for the industry. The differences in the welding performance between the infrared and blue lasers need to be clarified.

In the work, a high-power, up to 2000 W, blue laser welding system has been developed relying on the laser diode from Laserline GmbH. The potential of the blue laser for welding Cu-Al is explored. First, the high-power blue laser with different welding speeds was applied for the welding of Cu-Al sheets. Meanwhile, a high-speed camera is used to monitor and analyze the welding process. Second, the surface appearance, bead dimension, and element distribution are investigated based on the molten pool characteristics. Third, this work shows the mechanical and electrical properties with different process parameters. Finally, the key factors influencing the electrical property are discussed and the infrared and blue laser welding techniques are compared with each other.
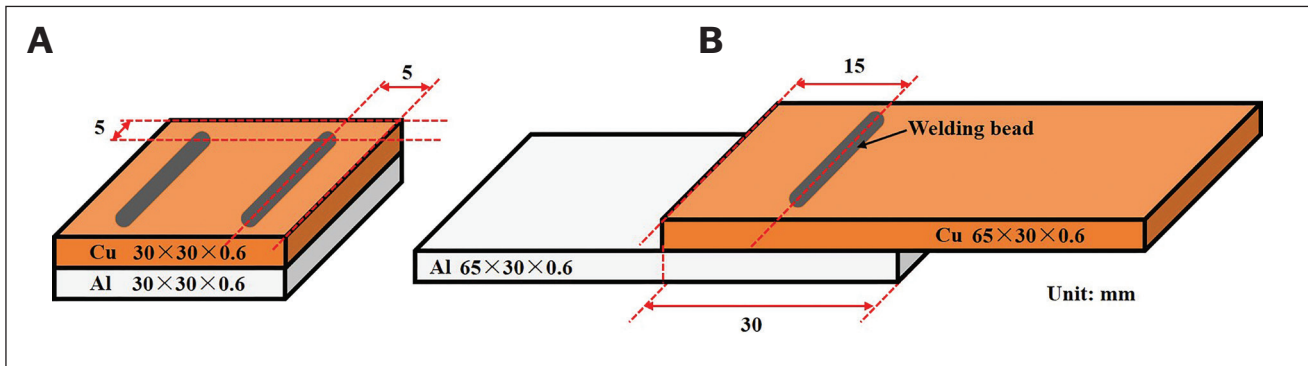
Fig. 2 — A — Sample for analyzing surface appearance and element distribution; B — sample for testing electrical and mechanical properties.
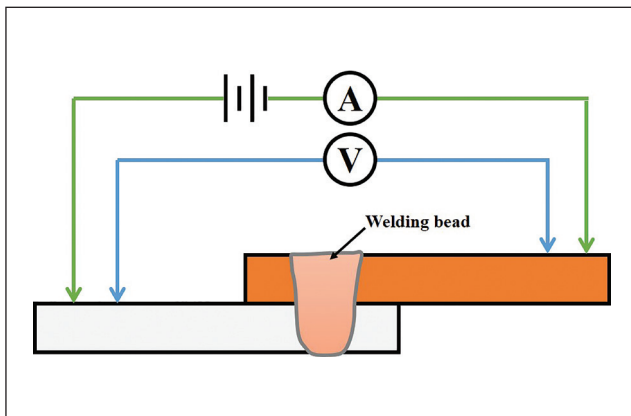
Fig. 3 — Sketch of the four-terminal sensing method for measuring the resistance.

Materials and Experiment Procedure

Experimental Setup

The experimental schematic diagram and photo of the blue laser welding system are shown in Fig. 1A continuous-wave semiconductor blue laser diode (LDMblue 2000-60 VG7H, Laserline GmbH, Mülheim-Kärlich, Germany) with a maximum power of 2000 W was used as the heat source for welding. The blue laser beam was delivered through an optical fiber of 600 μm in diameter from the laser diode and laser head. The wavelength range was 445 ± 20 nm. The distribution model of laser energy was a flat top. The specimens were fixed by a fixture to make sure there was no gap when welding, and the laser head moved through a three-axis displacement platform. When the blue laser beam focused on the substrate, the defocusing amount was 0 mm and the laser spot diameter was 0.6 mm. Argon was used as the shielding gas to prevent the oxidation of the molten pool and damage to the optical elements. Moreover, a high-speed camera (Revealer X213, AgileDevice Co., Ltd., Hefei, China) with 3000~5000 fps and 1.3 Mpix was applied to observe the welding molten pool. A laser light source and optical filter with 808 nm wavelength were utilized to avoid spectral interferences. An enlarging lens was used to enlarge the molten pool image 2 to 9 times.

Materials and Welding Procedure

In the blue laser welding Cu-Al experiment, the laser powers were 1500 and 1950 W, respectively. The welding speeds were 10, 20, 30, 40, and 50 mm/s, respectively. The maximum laser power of 1950 W with different welding speeds was applied to explore the blue laser welding limit capability. The length of the welding bead for every specimen was 20 mm. 0.6 mm commercially pure Cu sheet and 0.6 mm commercially pure Al sheet were overlapped for welding. The chemical compositions of commercially pure Cu and Al are listed in Table 1 and Table 2, respectively. Cu (T1) and Al (1050) were both typical specifications for battery applications in the new energy field. There were two sizes of specimens, including 30 mm × 30 mm × 0.6 mm and 65 mm × 30 mm × 0.6 mm, as shown in Fig. 2. The former was used for surface appearance and element distribution analysis; the latter was used to test electrical and mechanical properties. In addition, to clarify the formation reasons for the Cu-Al molten pool characteristics, the Cu-only and Al-only welds were carried out for molten pool observations with no other tests. The specimens for Cu-only and Al-only welds were both 2 mm thick to avoid welding through. Because the thicker specimen reduced the thermal accumulation effect which affected the molten pool characteristics, the molten pool images for Cu-only and Al-only welds were selected when the laser power was 1950 W, and the welding speed was 5 mm/s.

Characterization Methods

The welding bead surface was inspected by a laser scanning confocal microscope (VK-X3000, KEYENCE Co., Ltd., Shanghai, China) to obtain the color image and height image. The samples were cut by electron discharge machining in the middle of the welding bead perpendicular to the welding direction. The cross-section of the welding bead was ground by 80 to 2500 grade and was polished using 5, 1.5, and 0.5 μm diamond suspension solutions. Finally, metallographic corrosion was performed with Kohler's reagent. a metallographic microscope (Axio Imager .A2m, Carl Zeiss Microscopy GmbH, Jena, Germany) was applied to observe the cross-section. Meanwhile, the metallographic structure was analyzed by a Scanning Electron Microscope (SEM) (MAIA
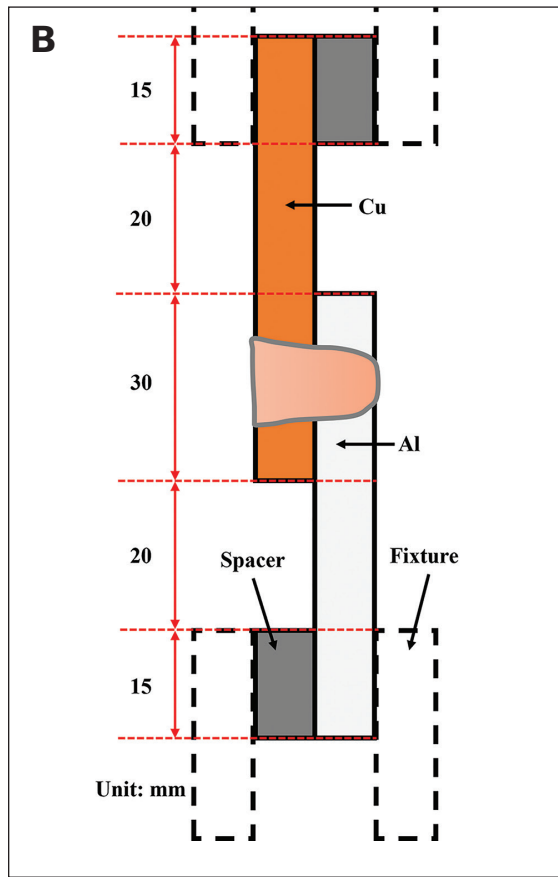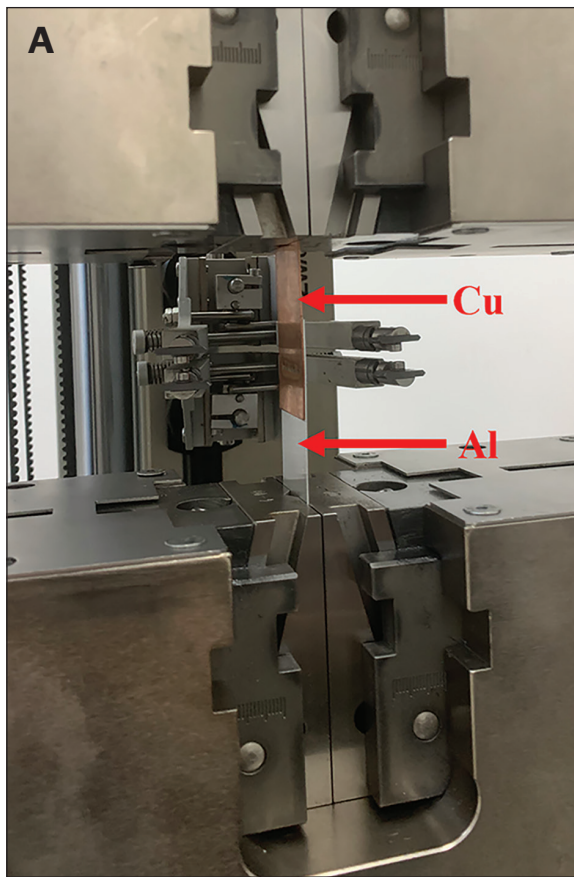
Fig. 4 — A — Experiment picture; B — schematic diagram of the shear force test.

3, TESCAN CHINA, Ltd., Shanghai, China) equipped with an energy-dispersive x-ray spectrometer (EDS).

Resistance value was a key electrical property in the welding of Cu and Al. The Kelvin four-terminal sensing method was used for resistance measurement, and the measurement sketch is shown in Fig. 3. Every data was measured nine times and averaged.

Shear strength is an important mechanical property. A universal testing machine (Roell Z100, Zwick Armaturen GmbH, Ennepetal, Germany) was applied to test the maximum shear force, as shown in Fig. 4. The test was implemented at the strain rate of 0.03 mm/min. Three repetitions were performed for each tested welding parameter.

Results

Molten Pool Characteristics

Molten pool characteristics can indicate the metallurgical behaviors that relate to the process mechanism (Ref. 19). These characteristics are the basis for analyzing the welding qualities and optimize process parameters. The molten pool images of Cu, Al, and Cu-Al are shown in Fig. 5. It can be found that there is a large grayscale region in the center of the Cu molten pool. The forming reason for the large grayscale may be the turbulent flow of liquid metal (Ref. 20). In addition,

the overexposure phenomenon has possibly appeared in the middle of the molten pool and is coincident with the laser spot. Depression accompanies overexposure, as shown in Fig. 5A. The main reason may be the production of plasma which leads to highlight and overexposure. Therefore, with the higher energy input, the above metallurgical behaviors are more evident. Compared with the Cu molten pool, there is no obvious grayscale change in the Al molten pool, as seen in Fig. 5B. The reason is that the metallurgical behavior of the Al molten pool is simpler than Cu molten pool. Due to the low blue laser absorptivity for Al, there is no possibility to generate a depression. But, for the Al molten pool, the melting slags and solidifying ripple are clear. The melting slags flow from the head to the tail, and during the solidifying process, the slags contribute to the ripple. The Cu-Al molten pool with Cu on top and Al on bottom can be considered as a combination of Cu and Al molten pool characteristics. The depression, overexposure, and slags all appear in Fig. 5C. With different welding penetrations, the Cu-Al molten pools have different characteristics. The detailed results and discussions will be exhibited in the following, together with the surface appearance and metallographic analysis.

Surface Appearance

The surface appearances, including confocal color images of the upper surface, confocal height images of the upper sur-
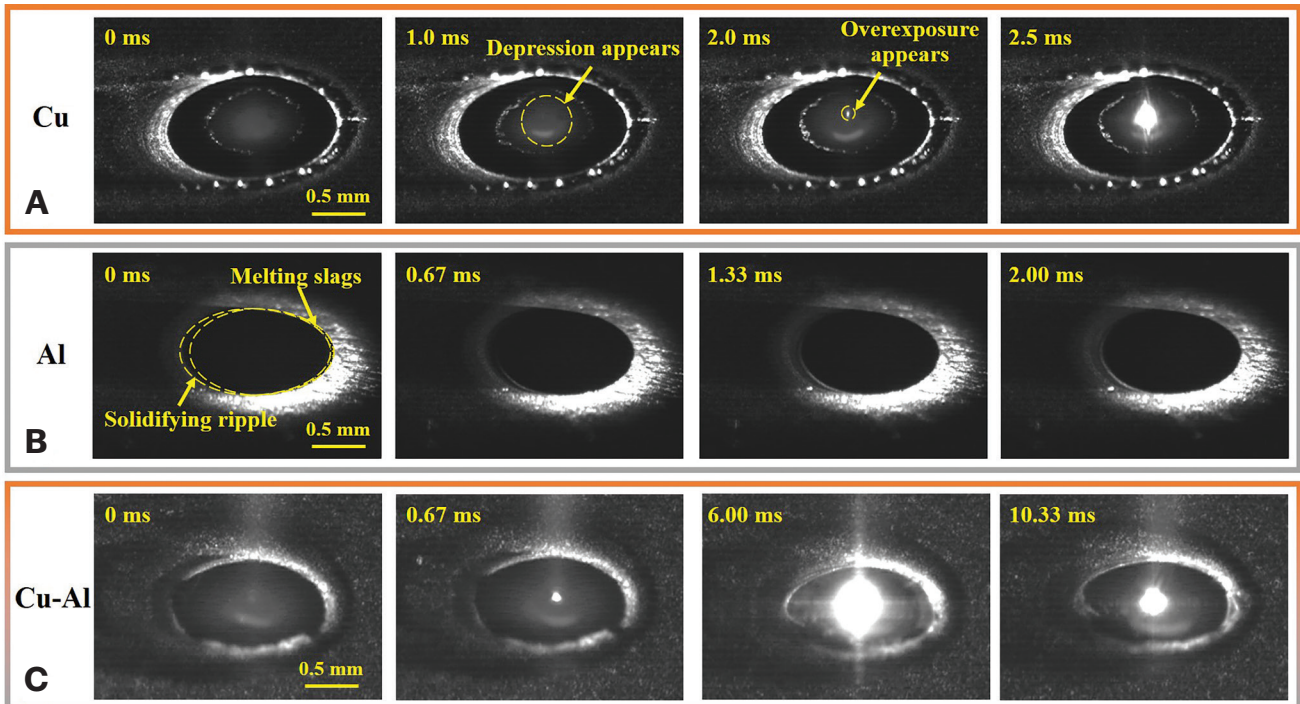
Fig. 5 — Typical molten pool characteristics of: A — Cu at 1950 W and 5 mm/s; B — Al at 1950 W and 5 mm/s; C — Cu on top and Al on bottom 1950 W and 20 mm/s.

Table 2 — Chemical Composition of Commercially Pure Al (1050)

Chemical Element	Al	Si	Cu	Mg	Zn	Mn	Ti	V	Fe
Mass Fraction (wt-%)	≥ 99.50	≤ 0.25	≤ 0.05	≤ 0.05	≤ 0.05	≤ 0.05	≤ 0.03	≤ 0.05	≤ 0.04

face, and color images of the bottom surface, with different process parameters, are displayed in Fig. 6. For the upper surface, the result shows that the larger laser power at 1950 W leads to a more unstable surface appearance with a larger surface roughness and a higher variation degree of welding bead width. There are six welding states ①~⑥ with different upper surface morphologies and molten pool characteristics. The first is that low-density Al fully floats to the surface of the molten pool with ultra-high energy input, as shown in Fig. 6①. In this situation, Al covers the surface of the welding bead which appears grey. Based on the molten pool image, it can be found that Al gathers along the edge of the molten pool, special for covering the molten pool tail. Figure 6② is the second state which has a cupreous upper surface. In this state, Al can float, but cannot cover the welding bead absolutely. The third state is like the second one but with a higher energy input, as seen in Fig. 6③. The higher energy input leads to a more violent oscillation. Therefore, the surface appearance in

the third has more roughness with mixed colors. Fig. 6④, ⑤, and ⑥ shows three states where the Al content decreases in turn. The substance with a large grayscale on the molten pool surface indicates the Al content. At the state ④, Al maintains to cover the surface. However, due to the low energy input, the slags are more obvious than that at the state ②. At the state ⑤, a little Al floats on the surface of the liquid Cu. At the state ⑥, the Al sheet on the bottom is not melted. There are no obvious large grayscale regions in the molten pool image.

For the bottom surface, the result shows that the regular upper surface can also result in an excessive melting bottom surface due to the low melting point of Al. Combining the appearances of the upper and bottom surface, the process parameters of 1500 W laser power with 20 mm/s welding speed and 1950 W laser power with 40 and 50 mm/s led to better welding qualities.
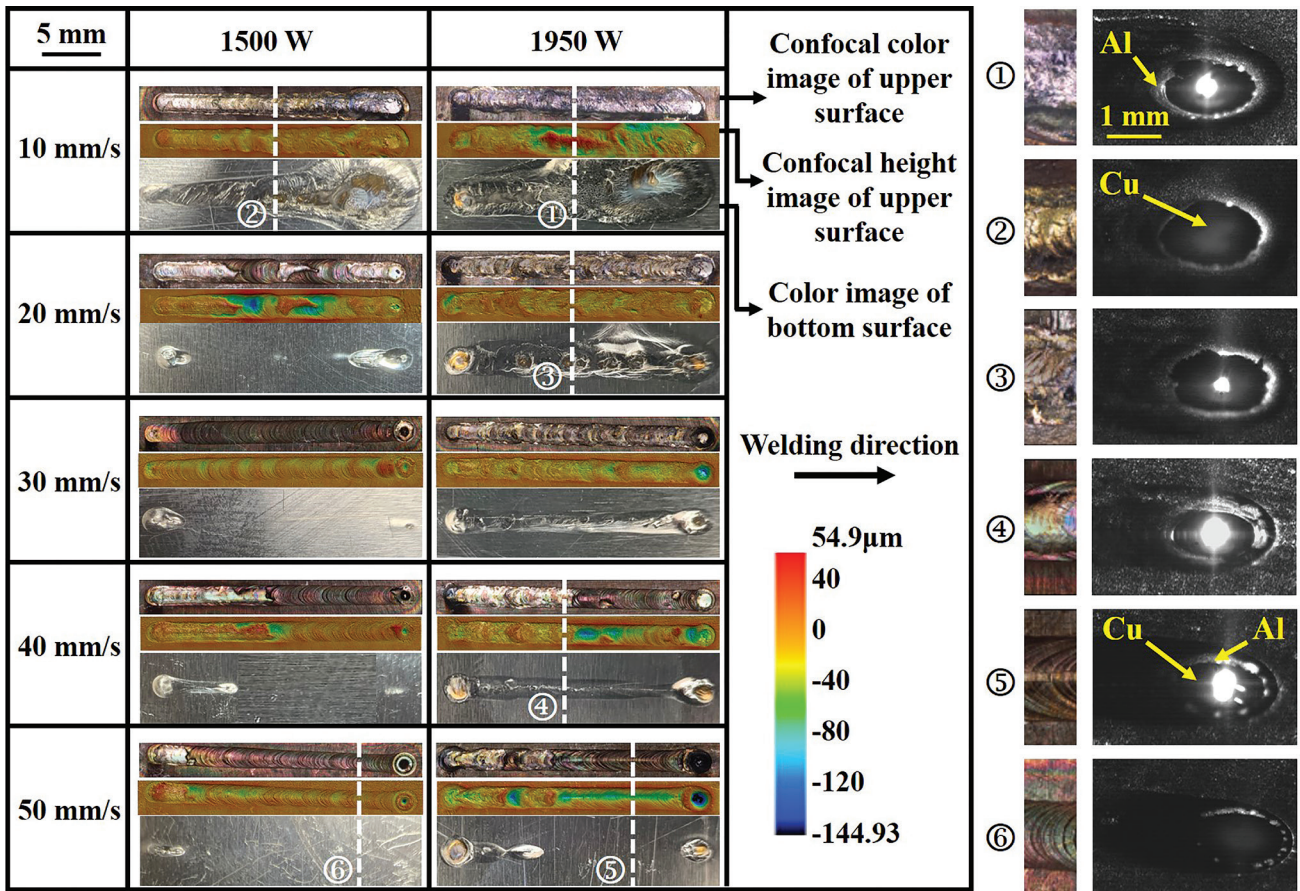
Fig. 6 — Surface appearance with different process parameters and typical molten pool characteristics with ①, ②, ③, ④, ⑤, and ⑥ welding states.

Cross-Section Image and Dimension

The cross-section images are shown in Fig. 7, which indicates that conduction welding is the main welding mode. Considering the six typical molten pool characteristics of Fig. 6, six different cross-section conditions can be achieved. Based on the results of the cross-section images and molten pool characteristics, the six welding states are listed as follows.

1. Condition ① — violence welding. The ultra-high energy input leads to the bottom layer Al melting completely and mixing with Cu. Due to the lower melting point of Al, the fusing region of the Al sheet is larger than that of the Cu sheet. The extremely violent welding state results in the generation of pores and cracks.

2. Condition ② — unstable welding. Because of the high energy input, the heat accumulation is very evident, and the molten pool temperature is very close to melting the bottom Al sheet. This is the state before going to condition ①.

3. Condition ③ — over welding. The energy input ensures that the Al sheet does not large area melt, resulting in many defects. However, the large penetration depth still welds through the Al sheet.

4. Condition ④ — good weld. A perfect welding result with appropriate penetration depths.
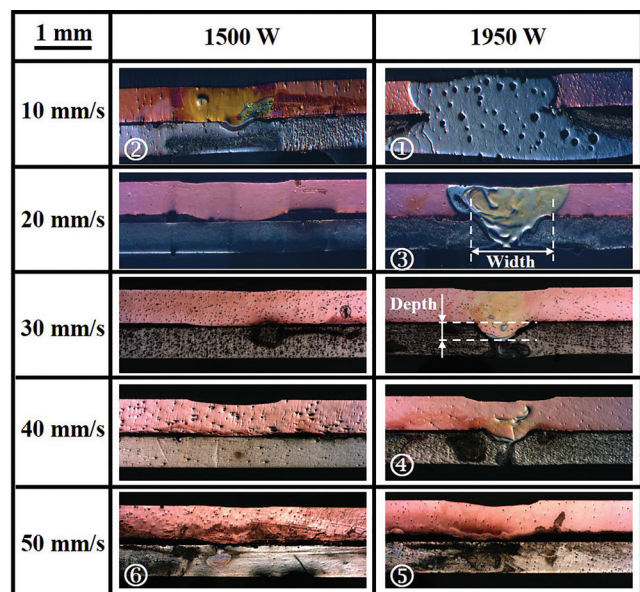
Fig. 7 — Cross-section images of welding beads with different process parameters.
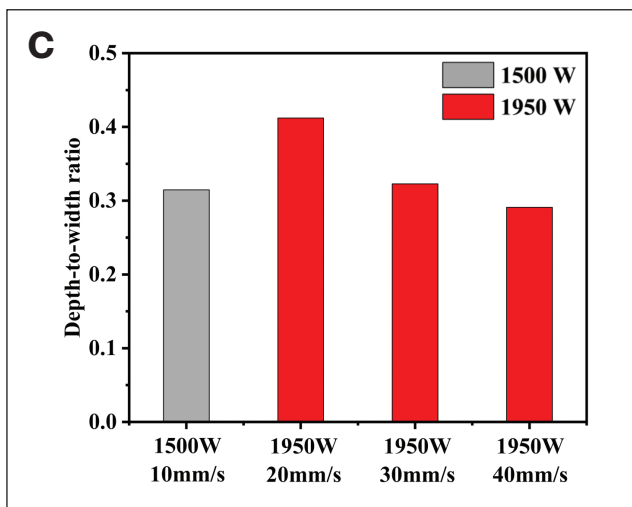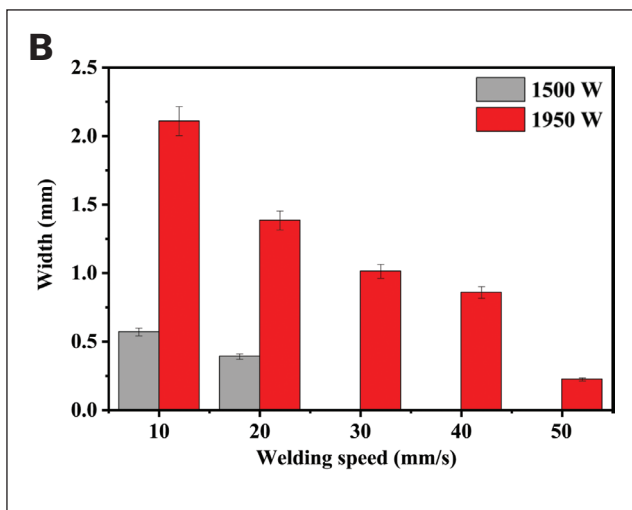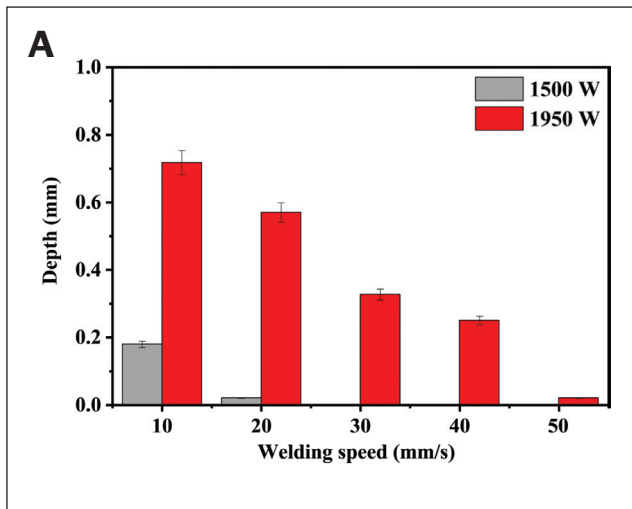
Fig. 8— Dimensions of welding bead with different process parameters: A —Depth; B — width; C — depth-to-width ratio.

5. Condition ⑤— lack of weld. Due to the small energy input, there is only a bit of join between the two sheets.

6. Condition ⑥ — no weld. There is no joint between Cu and Al sheets.

After obtaining the cross-section image, the welding bead dimensions are measured. The measuring positions and results are shown in Figs. 7 and 8, respectively. The results show that though the 1950 W laser power only increases by a third of 1500 W, the welding effect changes significantly. When welding with 1500 W at 20 mm/s to 50 mm/s, the bottom layer Al is difficult to join. If the welding speed decreases to 10 mm/s, the penetration depth can reach 0.18 mm. Even relying on the heat accumulation, the Al sheet can be completely penetrated as seen in Fig. 6. It indicates that there is a small process window when applying low laser power of 1500 W.

When applying the high laser power of 1950 W, the Al sheet is readily penetrated completely with the welding speed of 10 mm/s. The maximum welding width can reach 2.11 mm. With an increase in welding speed from 10 mm/s to 40 mm/s, the penetration depth, width, and depth-to-width ratio gradually decrease. When the welding speed is 40 mm/s, the depth and width of the welding bead can still achieve 0.25 and 0.86 mm, and the depth-to-width ratio is 0.29. The welding speed of 50 mm/s will reduce the penetration depth markedly.

Element Distribution

SEM images and Cu-Al element distribution at different process parameters are shown in Fig. 9. The result shows that a greater energy input can result in a more uniform mix of Cu and Al. Dimatteo et al. (Ref. 9) also found that the Cu sheet on top is more conducive to full fusion. When applying 2000 W blue laser welding Cu-Al, no matter whether it is 1500 W or 1950 W, the molten pool is at a relatively stable conduction welding state. The element distribution shows that low-density Al will flow upward from the center of the molten pool, while high-density Cu will flow downward in the center and carry out mass transfer to each other. In addition, there is an obvious transitional region between the welding bead and the substrate, which may be intermetallic compounds (IMC). Pfeifer et al. (Ref. 21) have demonstrated that the IMC could impact electrical resistance.

Mechanical Property

Shear force values with different process parameters are shown in Fig. 10. Because there are obvious welding defects in the bead when the speed is 10 mm/s, the samples with the welding speed of 10 mm/s are not tested. The result shows that there is an obvious gap between the samples of 1500 W and 1950 W. It means that, compared with the 1500 W blue laser power, the 2000 W blue laser power is very necessary from the point of view of mechanical properties. 2000 W blue laser power can greatly increase the allowable welding speed and enhance the welding efficiency.

When applying blue laser on welding 0.6 mm Cu and 0.6 mm Al sheets, the shear force of a 20 mm length welding bead can reach up to about 1000 N. Even though the welding speed is 50 mm/s, the shear force can still reach more than 600 N. One important reason for the large shear force per unit
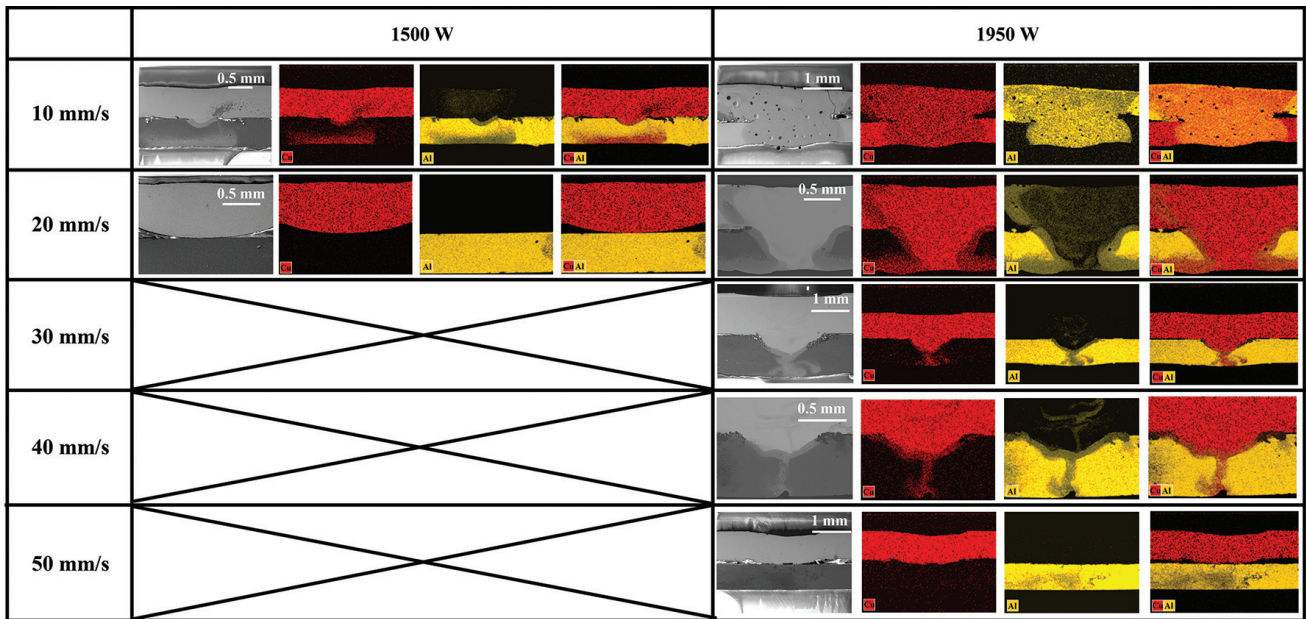
Fig. 9 — SEM images of the welding bead cross-section and the corresponding element distribution.
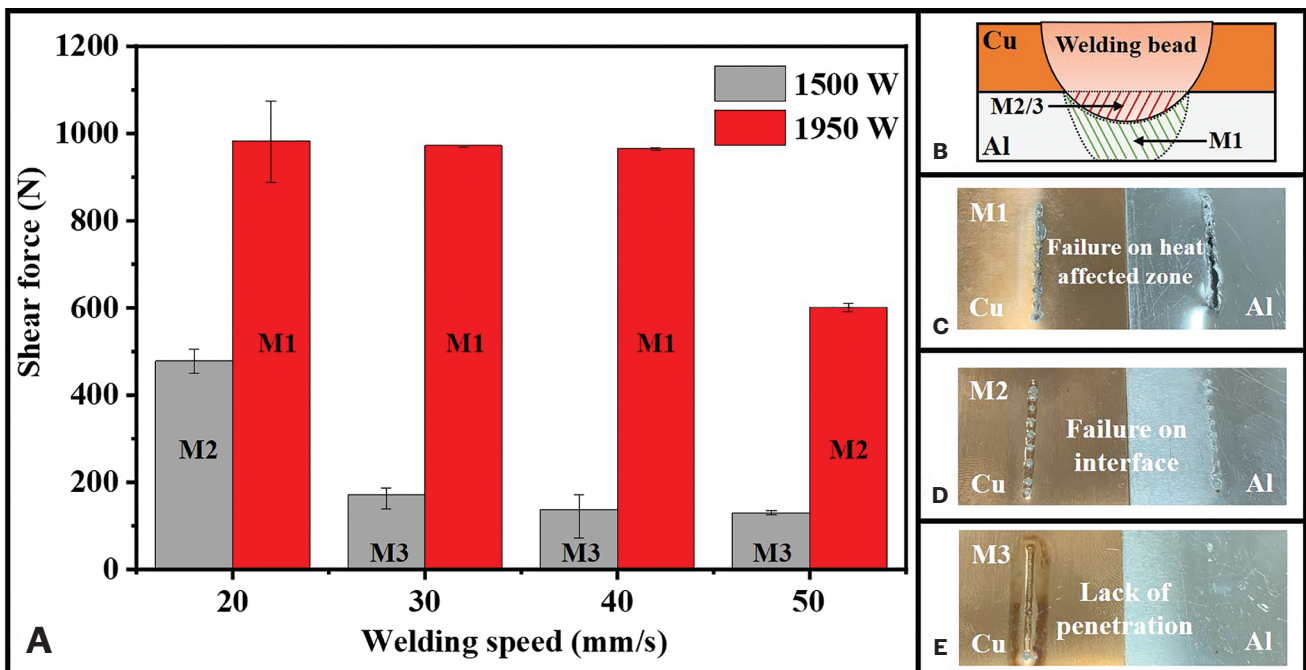
Fig. 10 — Shear force and failure modes of the samples with different laser powers and welding speeds: A — Histogram of shear force under different process parameters; B — fracture regions of different failure modes; C — fracture appearance of failure mode M1; D — fracture appearance of failure mode M2; E — fracture appearance of failure mode M3.

length compared with the infrared laser in references (Refs. 9, 22) is the large welding bead width resulting from the large spot diameter. The high absorption rate of the blue laser for Cu makes laser spot diameter welding possible. The fracture appearances of the welding beads are shown in Fig. 10. There are three failure modes based on the fracture appearance and shear force. The first failure mode M1 is caused by the tearing in the heat-affected zone or the Al substrate. Figure

10C shows the fracture appearance and Fig. 10B displays the fracture region. A large amount of weld structure remains on the Cu substrate. At the mode, the shear force is maximum and changes mildly with different welding speeds. One important reason is that the shear strength of the welding bead is large enough. Shear force relates to the phase composition and the property strength of the pure Al itself. The effect of process parameter variation is not significant. M2 is the second failure
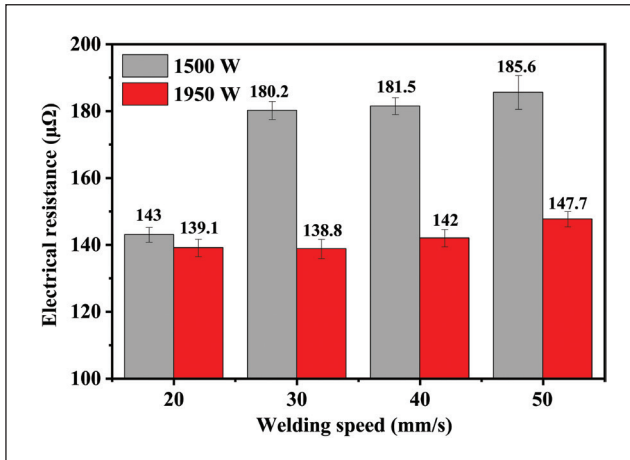
Fig. 11 — Electrical resistance values of the samples with different laser powers and welding speeds.

Fig. 12 — Schematic diagram of four key indicators when metallurgical behaviors change: The position of A is the potential overexposure region; B is the central region, C is the central region boundary; D is the external region; E is the molten pool tail.

mode in which the welding bead surface is uneven, as seen in Fig. 10D. The lack of mechanical properties of the welding bead causes the failure. When there is no metallurgical dilution at the Al sheet, the failure is owing to a lack of penetration as seen in M3 of Fig. 10E. The blue laser can hold the stability of the welding process and the high shear strength of the welding bead.

Electrical Property

Electrical resistance is a key electrical property in the joining of power batteries. Figure 11 shows the electrical resistance values of the sample with different laser powers and welding speeds. The results show that the larger energy input causes a lower electrical resistance. It means that more Al mixing into Cu and the larger welding bead makes it possible to achieve higher shear force while reducing resistance. When the welding speed is between 30 to 50 mm/s, the change in electrical resistance is not obvious. Therefore, a larger welding speed is acceptable for improving the efficiency in blue laser welding Cu-Al.

Discussion

Process Analysis Based on the Molten Pool Characteristics

Molten pool characteristics are the key to revealing the process mechanism and realizing feedback control. The basic molten pool characteristics of Cu, Al, and Cu-Al have been shown in Fig. 5. Based on the forming mechanisms of the molten pools when welding commercially pure Cu and Al respectively, the process when welding Cu-Al can be cleared. Six typical molten pools with different characteristics have been shown in Fig. 6. In these characteristics, there are four key indicators, as shown in Fig. 12. From the inside out, the key indicators are regions A, B, C, D, and E. A is whether the center region has been exposed. B is whether the outline of the center region is circular. C is whether the grayscale of the central region edge is large. D is whether there is an obvious high grayscale in the external region. E is whether the tail is covered by large grayscale slags. This is mainly related to the penetration condition and floating content of the bottom Al sheet in the molten pool. The floating process is exhibited in Fig. 13. Al floats through the center region and then gathers along the edge of the center region. With the increasing amount of Al, the Al continues to accumulate and cover the welding bead surface.
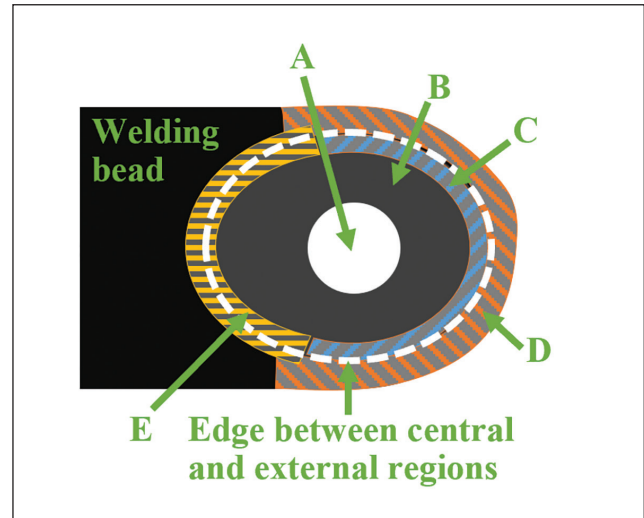
Six typical molten pool images and related qualities have been shown in Figs. 6 and 7 ①~⑥. The map is exhibited in Table 3. When almost no Al melts, the characteristics of the molten pool are almost identical to those of the Cu molten pool, as shown in Fig. 6 ⑥. Meanwhile, the energy input is low. Region A has no overexposure. When a little Al begins to float, because of the flow field, the Al will gather around the edge of the center region and raise the grayscale of region C in Fig. 12. The large energy input and relatively stable welding process result in continuous overexposure. The molten pool image can be seen in Fig. 6 ⑤. At this stage, the welding bead appearance gradually lightens from dark copper. Due to the inadequate welding depth, the mechanical and electrical properties are dissatisfactory. With the amount of floating Al, region C is covered by Al, and the grayscale increases, as seen in Fig. 6 ④. Obvious silver appears on the weld appearance. Silver means larger Al content. At this stage, the overexposure phenomenon is continuous with a stable outline of region B. These molten pool characteristics above at this stage indicate a good welding quality. When the energy input is enough high, Cu and Al mix on the molten pool surface, as exhibited in Fig. 6 ①, ②, and ③. The over and unstable process states lead to intermittent overexposure and unstable circular of region B. In addition, the amount of melting Al is large, and the Al is obvious by covering region E. Therefore, it can be concluded that the A-continuous overexposure, B-stable circular, C-large grayscale, D-large grayscale, and E-unobvious slags can indicate the well welding process and quality.
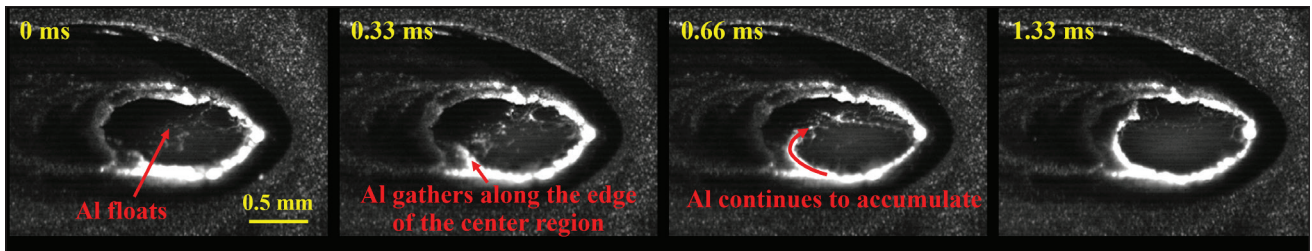
Fig. 13 — Floating process of Al.

On the one hand, it can be seen from the molten pool characteristics that the welding mode is still conduction welding when welding the 0.6 mm Cu and 0.6 mm Al sheets with the laser power at 1950 W. The welding process is overall excessively stable and has no splash, which is conducive to stable welding qualities. On the other hand, the quality repeatability of welding Cu-Al is still a great challenge owing to the strong heat accumulation and high thermal conductivity. There are also many different appearances in the same welding bead, as seen in Fig. 6. Therefore, if welding quality monitoring can be realized by using molten pool characteristics, it has important engineering application significance. Considering mechanical and electrical properties, it can be determined that the welding bead has better mechanical properties, electrical properties, and processing efficiency when Al floats up and covers regions C and D but does not spread to region E, and the central region B is stable with continuous overexposure of A. This metallurgical feature, combined with coaxial monitoring, can be used for real-time monitoring of the qualities of blue laser welding Cu-Al sheets.

Key Factors Affecting Resistance

Figure 14 draws the relationships between the resistance value and the other parameters. The results show that a larger shear force means a lower resistance value. It means shear strength and resistance value can be optimized simultaneously. It is quite different from welding with the form of Al on top and Cu on bottom. Pfeifer et al. (Ref. 21) studied the influence of IMC on electrical resistance. The result showed that the higher ratio of copper meant a higher resistance value. Therefore, when the Al is on the top, the higher energy input will lead to a higher ratio of Cu which increases the shear strength and decreases the electrical property. In addition, there is a limit value in both shear strength and resistance. It may result from the full fusion between Cu and Al when the laser power is large enough. Based on Figs. 10, 11, and 14, it can be found that the energy input is not a stable indicator to judge the processing state. Therefore, monitoring and back control is important.

Considering welding bead dimensions, the larger width indicates better electrical performance. One reason is the larger contact area. The other reason is the influence of the element distribution, in which the more thoroughly mixed leads to a lower resistance value. These experimental results show that, when using a high laser power at 1950 W, a larger energy input can obtain a better welding quality. It is opposite to the opinions in reference (Ref. 23), which presented that the more intensive mixing of Cu and Al led to the generation of IMC. The IMC had a higher resistance and impacted the electrical performance. The reason is that the blue laser has
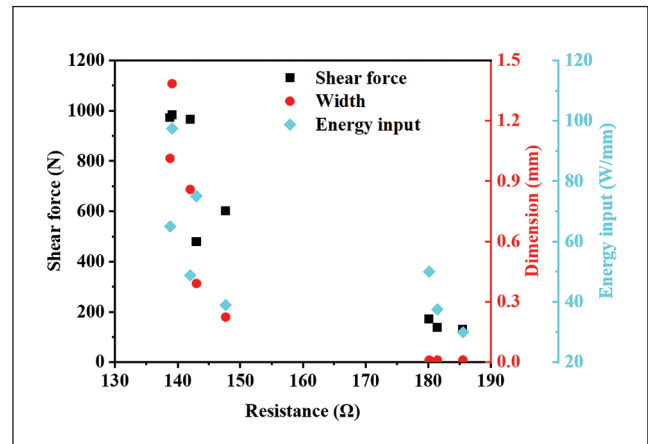
Fig. 14 — Relationships between resistance value and the other parameters: shear force, width, and energy input.

larger laser absorptivity and can weld in the form of Cu on top and Al on bottom. The form can mix Cu and Al more fully. When the energy input increases, the increasing Al content decreases the resistance. Meanwhile, in Fig. 9, the IMC thickness is inerratic between Cu and Al. Compared to a violent mix of the elements by the keyhole, as seen in (Ref. 7), the elements mixed in conduction welding resulting from the metal melting and mass transfer by Marangoni convection are more regular. Therefore, the stable IMC thickness and the welding form of Cu on top and Al on bottom result in that a larger energy input can obtain a better welding quality when there are no obvious welding defects.

Compared with Infrared Laser Welding of Cu and Al

Schematics of the mechanism in welding Cu-Al by an infrared laser and a blue laser are shown in Figs. 15A and B, respectively. When utilizing the infrared laser, for the high-reflection metal Cu and Al, large energy input and high energy density are necessary. At the moment, a keyhole will be produced to improve the absorption relying on multiple reflections and ensure the welding depth. Kawahito et al. (Ref. 24) have presented that the keyhole could raise the maximum absorption to 93%. Meanwhile, on the one hand, the keyhole is constantly changing which impacts the effect of multiple reflections, and then, makes the absorption vary. On the other hand, due to the high energy density, the plasma and metal vapor will generate and interfere with the laser radiation,
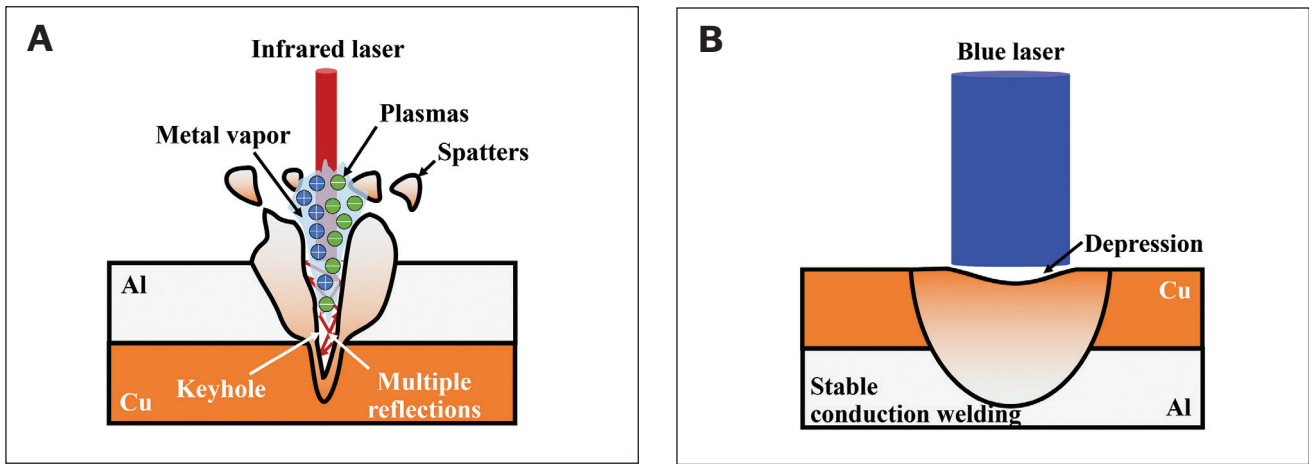
Fig. 15 — Schematics of the mechanism in welding Cu-Al by: A — An infrared laser; B — a blue laser.

Region	①	②	③	④	⑤	⑥
A-overexposure	intermittent	intermittent	intermittent	continuous	continuous	no
B-circular	unstable	unstable	unstable	stable	stable	stable
C-grayscale	large	large	large	large	large	low
D-grayscale	large	large	large	large	low	low
E-slags	obvious	obvious	obvious	unobvious	unobvious	unobvious

Table 3 — Mapping Relationships Between Region Characteristics and Quality Type

which drastically reduces the laser absorption. Therefore, the total laser absorption may fluctuate in the range of 5% (Ref. 1). Variational absorption, plasma, and metal vapor all make the keyhole welding process of the infrared laser unstable. For the blue laser welding of Cu, the laser absorptivity ratio can be greater than 60% (Refs. 25, 26). Therefore, dissimilar Cu-Al sheets can be processed by conduction welding with low energy density. In the conductivity welding mode, there is almost no splash and plasma, as shown in Figs. 5 and 6. It makes the welding process more stable.

For mechanical properties, this work has shown that the high laser absorptivity ratio can make the laser spot diameter available for blue laser larger and weld Cu-Al with the conduction mode. The large spot diameter with the conduction mode results in a large welding bead width which enhances the mechanical properties of the joint. For the electrical property, the computing method of the resistance factor is referred to (Ref. 9), in which the resistance factor with an infrared laser is near 1.0. When applying the blue laser, the resistance factor can reach down to 0.9, which has a bigger possibility to improve the electrical performance. Many factors influence electrical performance, which has been discussed in "Key Factors Affecting Resistance." One potential reason contributing to the improvement of electrical performance may be the larger cross-section area of the welding bead owing to the larger blue laser spot diameter. In addition, the high absorptivity of blue laser to Cu is beneficial to welding with the form of "Cu on top

and Al on bottom," which can mix Cu and Al more intensively and stably. On the one hand, it leads to a consistent IMC thickness with a wide range of process parameters. On the other hand, it makes the mechanical and electrical properties change in a similar trend when adjusting the process parameters. Therefore, compared with the infrared laser, the blue laser has potential in the field of new energy, such as the connection between the large thickness tabs of power batteries.

Conclusions

This work first realizes conduction welding of 0.6 mm Cu and 0.6 mm Al sheets using a 2000 W blue laser. The dynamic welding process, surface appearance, bead dimension, mechanical property, and electrical property of the welded sample are analyzed. The main conclusions are shown as follows:

1. A 2000 W blue laser can penetrate the dissimilar 0.6 mm Cu sheet and 0.6 mm Al sheet through stable conduction welding with no splash. A relatively good welding quality can be obtained with the laser power at 1950 W and the welding speed range from 20 mm/s to 40 mm/s.

2. There are six types of welding states with unique molten pool characteristics due to different Al content and energy input. The continuous overexposure, stable circular central region, large grayscale central region boundary and external region, and unobvious slags at the molten pool tail can be used

to indicate better qualities. It provides a possibility to control the welding quality.

3. Relying on the high absorption for Cu, the blue laser can carry out the Cu-Al sheets jointing by the conduction welding with the form of "Cu on top and Al on the bottom." This form makes the mechanical properties and electrical properties of the same change regulation. Meanwhile, the melting point of Cu is larger than that of Al. Both reasons lead to the idea that it is conducive to optimizing the welding process with a wider process window.

4. The blue laser results in a large bead width, a stable mass transfer state between Cu and Al, and a consistent IMC thickness. It is beneficial for performance improvement. The shear force of a 20 mm length welding bead can reach up to about 1000 N. The resistance factor can reach down to 0.9.

5. In the future, it is meaningful to compare the influence of conduction welding and keyhole welding with the infrared and blue laser on Cu-Al IMC and to analyze systematically the effects of these IMCs on the mechanical and electrical properties. The effect of blue laser in actual industrial processing should also be considered.

References

1. Yang, H., et al. 2022. Stable cladding of high reflectivity pure copper on the aluminum alloy substrate by an infrared-blue hybrid laser. *Additive Manufacturing Letters* 3: 100040.

2. Hong, K. M., and Shin, Y. C. 2017. Prospects of laser welding technology in the automotive industry: A review. *Journal of Materials Processing Technology* 245: 46-69.

3. Brand, M. J., et al. Welding techniques for battery cells and resulting electrical contact resistances. *Journal of Energy Storage* 1: 7-14.

4. Feve, J. P., et al. 2019. 500 watt blue laser system for welding applications. *High-Power Diode Laser Technology XVII*.

5. Bowman, R. L., et al. 1969. Solar absorptances and spectral reflectances of 12 metals for temperatures ranging from 300 to 500 K. *NASA Technical Note*.

6. Wang, H., Wu, Y. , and Wang, H. 2011. Current status of applying the blue laser in nonferrous metals processing. *The Chinese Journal of Nonferrous Metals* 31(11): 059–3070.

7. Hollatz, S., et al. 2020. Overlap joining of aluminum and copper using laser micro welding with spatial power modulation. *Welding in the World* 64(3): p. 513–522.

8. Jarwitz, M., et al. 2018. Weld seam geometry and electrical resistance of laser-welded, aluminum-copper dissimilar joints produced with spatial beam oscillation. *Metals* 8(7).

9. Dimatteo, V., Ascari, A., and Fortunato, A. 2019. Continuous laser welding with spatial beam oscillation of dissimilar thin sheet materials (Al-Cu and Cu-Al): Process optimization and characterization. *Journal of Manufacturing Processes* 44: 58–165.

10. Ascari, A., Fortunato, A., and Dimatteo, V. 2020. Short pulse laser welding of aluminum and copper alloys in dissimilar configurations. *Journal of Laser Applications* 32(2).

11. Nakamura, S., Mukai, T., and Senoh, M. 1994. Candela-class high-brightness InGaN/AlGaN double-heterostructure blue-light-emitting diodes. *Applied Physics Letters* 64(13): 1687–1689.

12. Nakamura, S., Mukai, T., and Senoh, M. 1994. High-brightness InGaN/AlGaN double-heterostructure blue-green-light-emitting diodes. *Journal of Applied Physics* 76(12): 8189–8191.

13. Tang, Z., et al. 2022. 2000W blue laser directed energy deposition of AlSi7Mg: process parameters, molten pool characteristics, and appearance defects. *Virtual and Physical Prototyping* 18(1): 2120405.

14. Brandau, B., et al. 2022. Absorbance study of powder conditions for laser additive manufacturing. *Materials & Design* 216: 110591.

15. Sadeghian, A., and Iqbal, N. 2022. Blue laser welding of low thickness Ni-coated copper and mild steel for electric vehicle (EV) battery manufacturing. *Optics & Laser Technology* 155.

16. Yuan, G., et al. 2022. Blue laser welding of 7075-T6 aluminum alloy and carbon fiber reinforced polyetheretherketone. *Optics & Laser Technology* 155.

17. Tang, Z., et al. 2023. Blue laser welding of laminated electrical steels: Dynamic process, weld bead characteristics, mechanical and magnetic properties. *Journal of Materials Processing Technology* 312: 117859.

18. Britten, S. W., et al. 2020. Blue high-power laser sources for processing solutions in e-mobility and beyond. *Procedia CIRP* 94: 592–595.

19. Tang, Z.-j., et al. 2020. Investigation on coaxial visual characteristics of molten pool in laser-based directed energy deposition of AISI 316L steel. *Journal of Materials Processing Technology* (290): 116996.

20. Tang, Z.-j., et al. 2020. Real–time prediction of penetration depths of laser surface melting based on coaxial visual monitoring. *Optics and Lasers in Engineering* 128: 106034.

21. Pfeifer, S., et al. 2012. Characterization of Intermetallic Compounds in Al-Cu-Bimetallic Interfaces. *Electrical Contacts (Holm), IEEE 58th Holm Conference on.*

22. Lerra, F., Ascari, A., and Fortunato, A. 2019. The influence of laser pulse shape and separation distance on dissimilar welding of Al and Cu films. *Journal of Manufacturing Processes* 45: 331–339.

23. Solchenbach, T., Plapper, P., and Cai, W. 2014. Electrical performance of laser braze-welded aluminum–copper interconnects. *Journal of Manufacturing Processes* 16(2): 183–189.

24. Kawahito, Y., et al. Laser absorption of aluminium alloy in high brightness and high power fiber laser welding. *Welding International* 26(4): 275–281.

25. Wang, H., et al., 2018. A model to calculate the laser absorption property of actual surface. *International Journal of Heat and Mass Transfer* 118: 562–569.

26. Wang, H., et al. Development of a high-power blue laser (445 nm) for material processing. *Optics Letters* 42(12): 2251–2254.

ZIJUE TANG, HUIHUI YANG, LE WAN, PENGYUAN REN, XIAOLIN ZHANG, YI WU, HAOWEI WANG, and **HONGZE WANG** (*hz.wang@sjtu.edu.cn*) are with State Key Laboratory of Metal Matrix Composites, Shanghai, China, and the School of Materials Science & Engineering, Shanghai Jiao Tong University, Shanghai, China. **WU, WANG,** and **WANG** are also with the Institute of Alumics Materials, Shanghai Jiao Tong University (Anhui), Huaibei, China. In addition, **WANG** is also with Anhui Province Industrial Generic Technology Research Center for Alumics Materials, Huaibei Normal University, Huaibei, Anhui, China.